Traffic Share-Based Multicast Scheduling for Broadcast Video Delivery in Shared-WDM-PONs

NamUk Kim, *Student Member, IEEE*, and Minho Kang, *Senior Member, IEEE*

***Abstract*—One of the important issues of convergence service design in access networks is its capability to provide an effective video delivery service for high-quality Internet Protocol television and multicast video on demand. In this paper, the authors research the effects of optical traffic sharing on convergence service design and address how to support multicast video delivery service with multicast scheduling in a shared wavelength division multiplexed–passive optical network (S-WDM-PON) which deploys a shared downstream wavelength and a broadcasting arrayed waveguide grating to a WDM-PON. The proposed dynamic channel scheduling mechanism, which is called maximum share first reservation (MSFR), and multicast management adjust transmission channel types based on the effective multicast cost of broadcast video so that the maximum number of videos can be delivered to homes by optical traffic share, while the packet processing burden and service interference among applications are reduced. The authors also discuss the network design issue regarding the optimal provisioning of shared link bandwidth to guarantee effective convergence services and economical efficiency of the network. The analysis and simulation results validate the effectiveness of the proposed mechanisms.**

***Index Terms*—Broadcast video delivery, multicast scheduling, passive optical network (PON), traffic share, wavelength-division multiplexing (WDM).**

I. Introduction

FORESEEING the growth of multimedia applications and the trend of service convergence, it is expected that wavelength-division multiplexed passive optical network (WDM-PON) will be an ultimate access network solution, even though time-division-multiplexed (TDM)-PONs are currently the focus due to their economic advantages that result from statistical multiplexing [1]–[3]. The WDM-PON provides an optical network unit (ONU) or an optical network terminal with a large link bandwidth by allocating a dedicated wavelength. As a result, it can guarantee a reliable performance that is required to support a triple-play-service (TPS) and service design flexibility, although optical system and device costs are still high [4]. To reduce network deployment cost and service granularity, some researches have proposed layered multiplexing methods such as a subcarrier multiplexing or TDM over WDM-PONs [5], [6]. Kim *et al.* [7] proposed a cost-effective WDM-PON that uses a downstream wavelength as an upstream carrier and also suggested types of network evolution scenarios and configuration models [8].

Manuscript received January 28, 2007; revised May 30, 2007. This work was supported by the Korea Science and Engineering Foundation (KOSEF) Grant funded by the Korean Government (MOST) under R11-2000-074-01001-0.

The authors are with Information and Communications University, Daejeon 305-732, Korea (e-mail: niceguy@icu.ac.kr; mhkang@icu.ac.kr).

Digital Object Identifier 10.1109/JLT.2007.902774

Irrespective of the benefits of these attempts to achieve a cost-effective solution, convergence services of TPS, including high-quality video, voice, and Internet data, must effectively be supported with a guaranteed quality of service (QoS) through a single data network of PON [4]. By considering the ever-increasing bandwidth demands of multimedia applications, it is not reasonable to try supporting convergence services with only a network engineering method of increasing the link speed, and traffic engineering mechanisms are evidentially required.

Broadcast video delivery for high-definition (HD) television, Internet Protocol television (IP-TV), and ordered multicast video is expected to be an important service in the near future. In data networks, this noninteractive video delivery is supported by multicast methods and affects the overall performance of TPS, even though interactive unicast and delayable videos are also important service models [9], [10]. The problem with a traditional broadcast video delivery comes from the fact that hundreds of video streams must be transmitted through a single data network during a long service sojourn time. In cable networks, the entire broadcast videos are constantly delivered to a home set-top-box (STB), with only some videos selected by the customers. By considering the large bandwidth occupation of HD video content, the delivery of the entire videos is not an effective solution for PONs. Perkins *et al.* [11] showed that the link bandwidth that is needed to deliver an HD video through the IP network increases rapidly as the image quality goes up. Although video compression technologies or high-order digital modulation can reduce the bandwidth necessary for a video [12], [13], it is still difficult to deliver hundreds of HD videos, guaranteeing the QoS of all the applications. Moreover, modification of the system configuration and modulation techniques is inevitable whenever the required image quality of broadcast video increases, and service efficiency is always low because only a few videos are utilized among the delivered videos.

Meanwhile, most video servers can deliver only the videos requested by the customers by the use of multicast technologies. This minimizes unnecessary bandwidth provisioning, but maintaining the sharing of videos in the distribution network from the optical line termination (OLT) to the ONUs is difficult due to the point-to-point architecture of the WDM-PON. On the other hand, TDM-PONs such as E- and G-PONs can effectively support broadcast video delivery by using an optical packet broadcasting property that is achieved using a point-to-multipoint network architecture [2]. However, due to the limited link bandwidth and single shared link, it is hard to fully support broadcast videos without a serious service interference among applications. By considering the ever-increasing multicast video applications, optimal broadcast video delivery is a

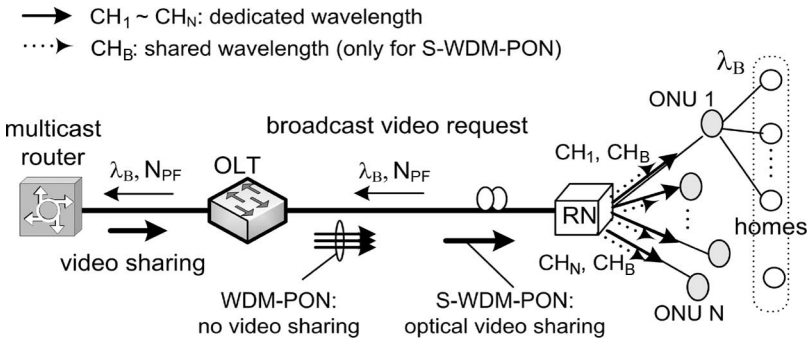

Fig. 1. Broadcast video delivery over WDM-PON.

primitive requirement in the design of a convergence service that is independent of a current link bandwidth.

In this paper, the properties of a broadcast video delivery and the effects of a multicast traffic sharing on the performance of convergence services are analyzed. The proposed TPS-centric shared WDM-PON (S-WDM-PON) architecture and multicast scheduling mechanism, which is called the maximum-share-first-reservation (MSFR) mechanism, aim to effectively support convergence services by achieving a maximum traffic share in the optical layer and optimal bandwidth allocation for the types of applications that are used for changes in broadcast video demand. The design issue regarding optimal provisioning of a shared link bandwidth to guarantee effectiveness of convergence services and economical efficiency of a network is also dealt with.

The remainder of this paper is as follows. The architecture of the S-WDM-PON and the properties of a broadcast video delivery are explained in Section II. Section III describes the multicast management operations and proposes an adaptive multicast scheduling mechanism. The effectiveness of sharing a video virtual channel is analyzed, and the overall performance of the proposed mechanism is validated in Section IV. Section V concludes this paper.

II. Shared WDM-PON Architecture

A. Broadcast Video Delivery in PONs

It is evident that some broadcast videos have a tendency to be requested more frequently than others in a broadcast video repository. The probabilistic distribution of these preference (hot) videos affects multicast traffic share. Based on the Zipf distribution which models the more or less concentrated access pattern of multimedia content service [14], the request probability for a broadcast video j is derived as

$$p_j = \frac{C}{j^{\alpha}}, \qquad C = \frac{1}{\sum_{j=1}^{N_{\mathrm{BV}}} 1/j^{\alpha}} \tag{1}$$

where N_{BV} denotes the total number of broadcast videos in the video repository. Following the normal video borrowing model [14], the value of parameter α is assumed to be one in this paper. By the video request probability of (1), broadcast videos can be ordered from videos 1 to N_{BV} so that p_i is larger than p_{i+1}, and the average video request rate of video j is equal to $\lambda_j = \lambda_B \cdot p_j = \lambda_B \cdot C/j$, where λ_B is the total broadcast video request rate in the video server. Our discussion is on the average broadcast video share for λ_B and its pattern.

Based on the ordered average video access rates, broadcast videos can be divided into two sets. The first set consists of N_{PF} preference video requests, which can be combined due to a plurality of requests during video play time. This set begins with video 1 and ends with video N_{PF}. The videos of the second set are cold videos that are requested by equal or less than one home. This set begins with video $N_{\mathrm{PF}+1}$ and ends with N_{BV}. Thus, if a broadcast video j is a preference video with playtime L_j, $\lambda_j \cdot L_j$ is larger than one. In this paper, for simplicity, it is assumed that L_j is equal to L. Thus, the fraction of video requests to preference videos (ρ_{PF}) is yielded as [15]

$$\rho_{\mathrm{PF}} = \frac{\sum_{j=1}^{N_{\mathrm{PF}}} \lambda_j}{\sum_{j=1}^{N_{\mathrm{BV}}} \lambda_j} = \frac{\sum_{j=1}^{N_{\mathrm{PF}}} 1/j}{\sum_{j=1}^{N_{\mathrm{BV}}} 1/j} = \sum_{j=1}^{N_{\mathrm{PF}}} C/j. \tag{2}$$

If the video server supports broadcast video delivery with multicast protocol such as Internet group management protocol (IGMP), requests for the same preference video can be supported by a single video virtual channel, which is the guaranteed link bandwidth that is required to deliver a video. As a result, the number of necessary video virtual channels is derived as

$$\sum_{i=1}^{N_{\mathrm{PF}}} \frac{L}{T} + (1-\rho_{\mathrm{PF}}) \cdot \lambda_B \cdot L = N_{\mathrm{PF}} \cdot \frac{L}{T} + (1-\rho_{\mathrm{PF}}) \cdot \lambda_B \cdot L \tag{3}$$

where T is the video playtime interval. In this paper, L is assumed to be the same as T, i.e., a single video service period, and hereafter, λ_B represents the normalized arrival rate of video requests during L. Thus, the amount of link bandwidth that is necessary between the server and the OLT is achieved as

$$\mathrm{BW}_{\mathrm{server}}(N_{\mathrm{PF}}, \lambda_B) = S_B \cdot (N_{\mathrm{PF}} + (1-\rho_{\mathrm{PF}}) \cdot \lambda_B) \tag{4}$$

where S_B is the video virtual channel bandwidth. Conversely, broadcast video sharing cannot be achieved from the OLT to the ONUs in WDM-PONs since preference videos are transmitted by dedicated wavelengths of member ONUs. Thus, the number of video virtual channels is always equal to the number of member ONUs, and the necessary link bandwidth is much larger than $\mathrm{BW}_{\mathrm{server}}(N_{\mathrm{PF}}, \lambda_B)$, as shown in Fig. 1. On the contrary, TDM-PON supports video sharing with optical packet

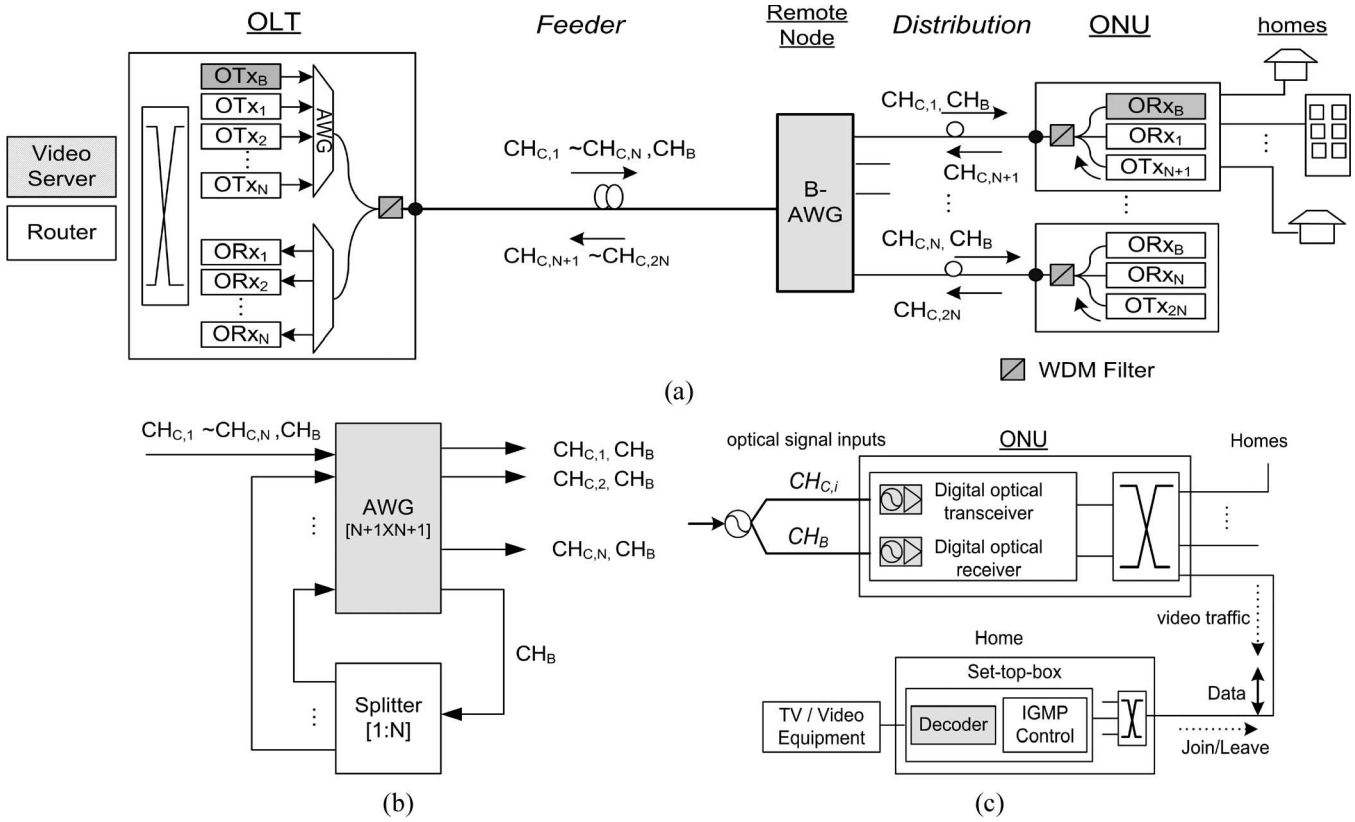

Fig. 2. Architecture of the S-WDM-PON and configuration of a node. (a) Overall S-WDM-PON architecture. (b) Configuration of B-AWG in an RN. (c) Configuration of ONU and home for data communication and broadcast video delivery.

broadcasting, but a stable traffic isolation is not guaranteed due to a single shared link and limited bandwidth, as discussed.

B. Architecture of the S-WDM-PON

1) Network Architecture: The overall architecture of the S-WDM-PON is shown in Fig. 2(a). The topology consists of a single-fiber feeder and a star topology distribution network for N ONUs. The S-WDM-PON deploys a shared downstream channel (wavelength) to the WDM-PON. Thus, two different kinds of downstream data channels and a single upstream channel are provisioned. $\mathrm{CH_B}$ is a shared downstream channel that is supposed to deliver a multicast traffic. Through an optical power splitter (OPS) deployed in a remote node (RN), packets transmitted by $\mathrm{CH_B}$ are optically split and delivered to all ONUs. The OLT also allocates a dedicated data channel $\mathrm{CH}_{C,i}$ to the ONU_i by arrayed waveguide grating (AWG). Thus, the OLT has $N+1$ distributed feedback lasers (fixed transmitter) for the downstream transmission and N optical filters (fixed receiver) for receiving upstream traffic, where each laser and filter pair is dedicated to a single ONU.

Correspondingly, the ONU_i has two fixed optical filters tuned to $\mathrm{CH_B}$ and $\mathrm{CH}_{C,i}$, and a single laser. The optical signals, including the broadcast channel, are fed to the input port of a broadcasting AWG (B-AWG), where optical signals are routed to the output port to the destination to which the ONU is connected [16].

2) Node Architecture: The B-AWG is made up of a cyclic AWG and an OPS, as shown in Fig. 2(b). A loop-back configuration optically connects the last output port to the input ports through the power splitter to ensure that the broadcasting wavelength $\mathrm{CH_B}$ can be routed to every node in a cyclic way. At each node, incoming optical signals are demultiplexed by a WDM filter and are received by a photodiode that is connected to its output ports. As the signal power of the shared wavelength is split, the power budget can be a problem, but the calculation of power based on commercial devices shows enough power margin for a normal split ratio in access networks, which is $16:1$ [17]. The performance of the device that is deployable in the S-WDM-PON is similar to that of a normal overlay WDM-PON [13], [17]. If $\mathrm{CH_C}$s and $\mathrm{CH_B}$ are selected from the C- and L-band spectrums, the power losses of commercial devices are listed as follows [17]: fiber loss $= 0.25$ dB/km, AWG $= 5$ dB, coupler loss $= 13$ dB $(1:16)$, and CWDM filter $= 1$ dB. Thus, to satisfy a receiver sensitivity at 1 Gb/s [-26 dBm (PIN) and -36 dBm (APD)] and network coverage $= 20$ km, the required transmitter power for $\mathrm{CH_C}$ is -7 dBm and -17 dBm for PIN-PD and APD, respectively. Meanwhile, the transmitter power for $\mathrm{CH_B}$ increases to 11 and 1 dBm, due to signal splitting and the loop-back second stage AWG. If the split $\mathrm{CH_B}$ is not again fed to the AWG by connecting it to the ONU directly, the 5-dB loss can be decreased [17]. The split ratio and the coverage distance can be increased by increasing the transmitter power of $\mathrm{CH_B}$ in the OLT or by amplifying the signal in the path of $\mathrm{CH_B}$ [18].

The power budget problem has also been a critical issue in TDM-PONs. Thus, evolutionary laser technologies or preamplifiers developed in TDM-PONs can also be applied to the

proposed architecture to accommodate more ONUs since the deployed shared wavelength configures the same logical TDM-PON [18]. Alternatively, it is possible to deploy an optical amplifier at the shared output port in the B-AWG to increase the split ratio. Even though the system cost and entire capital expenditure (CAPEX) may increase, the cost per customer eventually decreases since the OLT can support more customers [19]. The effectiveness of broadcast video sharing increases as the number of customers in the S-WDM-PON increases, which is the major subject of this paper and will be validated in the following sections.

The logical architecture of the ONU is shown in Fig. 2(c). In this paper, a fiber-to-the-curb (FTTC)-type WDM-PON, which is an alternative PON in reducing CAPEX of network deployment, is assumed. First, the ONU receives the digital input signal and converts it to a data frame. Next, packets are switched to their destination homes by the destination address and the types of packets. Last, video packets are converted to the appropriate video signal in an STB and are delivered to the video equipment. Video selection can be controlled by an IGMP control unit with an application such as an electric program guide, which is the solution for IP-TV [20].

The configuration of the OLT or the ONU can be replaced by another device combination such as a continuous wavelength or loop-back transmission module to achieve a more cost-effective network. This overlay wavelength assignment has been researched to support the delivery of the entire videos by the use of a broadband light source or to guarantee ONUs different QoS for burst traffic [13], [17]. However, the objectives of shared channel provisioning are different from the objective of this paper, which aims to achieve an effective broadcast video delivery with optimal traffic share and bandwidth allocation, i.e., optimal traffic engineering. Note that the proposed algorithm and numerical analysis can be applied to any kind of overlay WDM-PON, regardless of the differences of node or device configuration.

C. Multicast Management in the OLT

The multicast management of the OLT for broadcast video delivery makes use of the aforementioned features of S-WDM-PON. In the following sections, first, the principles of downstream packet transmission are explained, and then, the operation of multicast channel scheduling is described.

1) Underlying Principle: Due to the fact that the two kinds of downstream channels have different topological configurations, the OLT has to determine the downstream channel of the packets. There are three basic operational principles by which the control of broadcast video delivery is supported in the S-WDM-PON.

1) The broadcast video server delivers only the broadcast videos requested by customers to the OLT with IGMP, and the OLT maintains the multicast management information of all multicast groups (MGs), i.e., broadcast videos being delivered to itself, through the use of IGMP snooping [21], [22].
2) The OLT configures MGs for broadcast videos based on the logical output ports of $\mathrm{CH_C}$s connected to the corresponding ONUs by parsing the JOIN or LEAVE messages to make sure that port-based multicast switching is always supported [22].
3) The multicast agent of the OLT adaptively determines the transmission channel of the MG by using a multicast scheduling mechanism. Channel information is recorded in the MG management table (MGMT) and is referenced by the switch block.

Based on the aforementioned principles, the OLT checks the type of incoming packet by parsing the destination IP or MAC address using the ingress rule, as shown in Fig. 3. In the case of the Ethernet, a multicast destination address is generated by an MG IP and reserved bit sequences $0\times$01-00-5E [22]. If the packet is a unicast packet destined to the ONU_i, the OLT switches it to the logical port of $\mathrm{CH}_{\mathrm{C},i}$, which is connected to ONU_i. The channel types of broadcast videos are adjusted by the scheduling algorithm to achieve optimal video share through $\mathrm{CH_B}$. The multicast agent of the OLT also snoops all the multicast control messages and updates managed information elements of the MGMT.

2) Multicast Management Operation: In this paper, the objective of the multicast management is to achieve an optimal broadcast video share through a shared channel, regardless of the change in multicast membership. Using multicast protocol, each broadcast video that is delivered to the ONUs is managed as an MG in the MGMT, as shown in Fig. 3(a), where MG_j consists of four managed information bases.

1) $\mathrm{CT}[\mathrm{MG}_j]$—channel type: CT indicates the data channel type by which packets of the MG are transmitted. The index S represents a shared $\mathrm{CH_B}$, and D represents the dedicated $\mathrm{CH_C}$s of member ONUs of MG_j.
2) $\mathrm{SI}[\mathrm{MG}_j]$—share-index: The number of member ONUs which have currently joined the MG_j. The multicast agent of the OLT increases or decreases the value of SI by one whenever an ONU joins or leaves the MG_j.
3) $\mathrm{S_B}[\mathrm{MG}_j]$—virtual channel bandwidth: Guaranteed link bandwidth of a video virtual channel that is required to deliver multicast packets of MG_j stably.
4) MG pointer: The MG pointer indicates the port-based MG table that registers member ONUs based on the logical ports of $\mathrm{CH_C}$ from which the JOIN or LEAVE message arrives. The Ethernet virtual local area network (VLAN) or IGMP of commercial switches can be used to configure an MG table.

The information that is necessary to manage MGMT can be informed using a multicast block of switch. The packet switching and transmission schemes discussed earlier are shown in Fig. 3(b). An incoming multicast packet of MG_j is switched based on the referenced $\mathrm{CT}[\mathrm{MG}_j]$ information. If it is S, the packet is directly delivered to the logical port of $\mathrm{CH_B}$, apart from the switching path. In the opposite case, it is delivered to the logical ports of $\mathrm{CH_C}$s of member ONUs with the use of multicast switching. We note that this overlay delivery guarantees the ONUs broadcast video sharing in the optical layer, and a multicast agent has to guarantee an optimal bandwidth allocation for maximum video share through $\mathrm{CH_B}$.

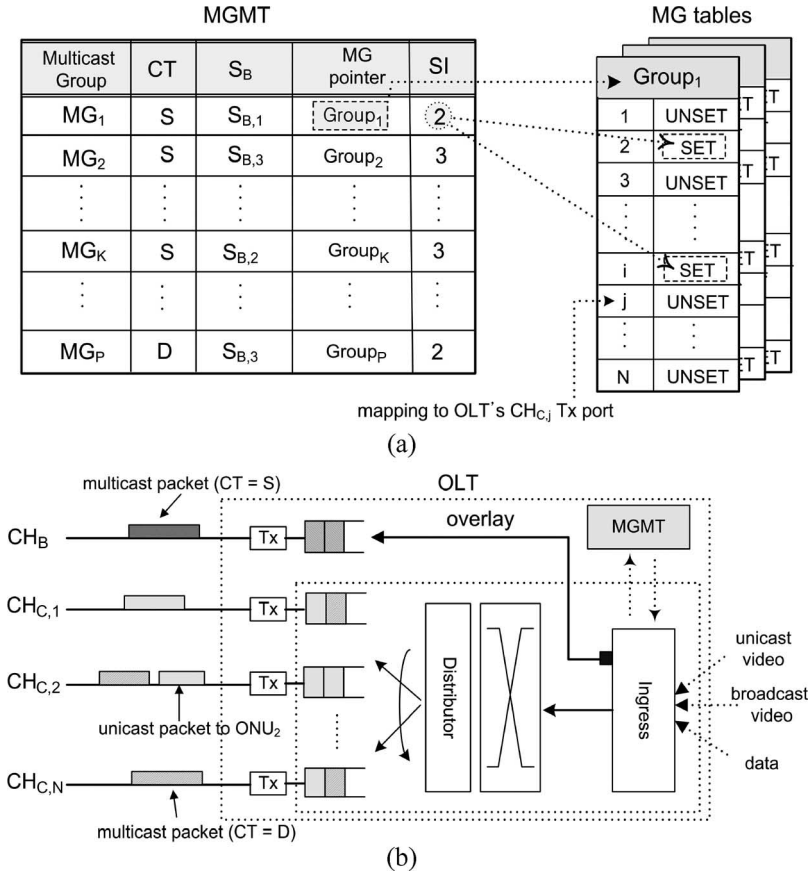

Fig. 3. Overlay broadcast video delivery. (a) Configuration of MGMT and MG management. (b) Packet switching and transmission.

The most straightforward multicast scheduling for the control of virtual channel reservation is the first-come-first reservation (FCFR) mechanism. It sets CT $= S$ until there are no more allocable virtual channels in $\mathrm{CH_B}$, and then, the excess broadcast video requests are supported by $\mathrm{CH_C}$s connected to member ONUs. The FCFR guarantees a fair link sharing, and several broadcast videos can optically be shared. However, preference videos are randomly distributed over $\mathrm{CH_B}$ and $\mathrm{CH_C}$ since the channel types of broadcast videos are determined by the video request load at the time of virtual channel reservation. Therefore, if the bandwidth of $\mathrm{CH_B}$ is entirely allocated, the heavy-joined MGs of a large SI must be delivered by $\mathrm{CH_C}$s, and a large link bandwidth is needed. To achieve an effective broadcast video delivery, it is required to maintain a maximum traffic share through $\mathrm{CH_B}$, which is independent of the change in broadcast video demands or network load.

III. Optimized Broadcast Video Delivery

A. Problem Definition

The constraints of video virtual channel allocation for broadcast videos can be described as follows [23]:

$$\sum_{i=1}^{N_B(t)} S_B[\mathrm{MG}_j] \le W \tag{5}$$

$$P_B \le P_{G,B}, P_R \le P_{G,R} \tag{6}$$

where $N_B(t)$ is the number of broadcast videos that are delivered to the ONUs by $\mathrm{CH_B}$ at time t. The blocking loss rate of the broadcast video $(P_{G,B})$ and real-time unicast video $(P_{G,R})$ must be strictly guaranteed. With a shared link $\mathrm{CH_B}$ that has a bandwidth of W, each ONU is provided with an average of W/N additional link bandwidth. However, the effective bandwidth and throughput of the ONU differs in multicast traffic sharing. For example, if an ONU joins preference videos that are delivered to other ONUs by $\mathrm{CH_B}$, the effective throughput of the ONU is larger than $W + W/N$, while no channel reservation contention or additional link bandwidth allocation occurs. Note that, in this case, the effective allocable bandwidth of an ONU (the resultant throughput of the ONU) increases in proportion to the requests of preference videos.

In WDM-PONs, the number of video virtual channels of $\mathrm{CH_C}(m_B)$ that is necessary to deliver C_B broadcast videos with an average request rate of $\lambda_{B,\mathrm{ONU}}$ (requests from homes in a single ONU segment) can be derived as [15]

$$m_B = \min\left\{ k \left| \frac{\left(\frac{\lambda_{B,\mathrm{ONU}}\cdot C_B}{\mu_B}\right)^k \cdot P_0}{k!\left(1-\frac{\lambda_{B,\mathrm{ONU}}\cdot C_B}{k\cdot\mu_B}\right)} < P_{G,B} \right.\right\}$$

$$P_0 = \left[\sum_{n=0}^{k-1} \frac{\left(\frac{\lambda_{B,\mathrm{ONU}}\cdot C_B}{\mu_B}\right)^n}{n!} + \frac{\left(\frac{\lambda_{B,\mathrm{ONU}}\cdot C_B}{\mu_B}\right)^k}{k!\left(1-\frac{\lambda_{B,\mathrm{ONU}}\cdot C_B}{k\cdot\mu_B}\right)}\right]^{-1} \tag{7}$$

where μ_B is the average service rate of a single broadcast video, and k is a dummy variable. Conversely, it is possible to support a plurality of broadcast video requests for a preference video with a single virtual channel in the S-WDM-PON. If $m_{\rm sh}$ is the average number of shared broadcast videos destined to an ONU and $\rho_{\rm sh}$ is the ratio of the total requests to those shared videos, (7) is modified as $\lambda_{B,\rm ONU} \rightarrow \lambda_{B,\rm ONU} \cdot (1-\rho_{\rm sh})$ and $C_B \rightarrow C_B - m_{\rm sh}$. Thus, the value of m_B decreases as $m_{\rm sh}$ and $\rho_{\rm sh}$ of $\rm CH_B$ increase.

The effects of broadcast video sharing are not simply proportional, and its effectiveness is maximized at peak time. The performance of the OLT system in terms of the packet processing burden and buffer can also be improved by the deflected switching. Thus, the functional requirements of multicast channel scheduling can be summarized as follows.

1) The number of preference videos that are delivered by $\rm CH_B$ must always be maximized, which is independent of the time of virtual channel reservation or change of network load.
2) The number of member ONUs which join the preference videos that are delivered by $\rm CH_B$ must be maximized.
3) The amount of broadcast video traffic, which is optically shared by the ONUs, must be maximized.

To achieve the aforementioned requirements, the multicast agent has to adaptively adjust the channel types of broadcast videos for the changes in user broadcast video demand and traffic sharing and to reallocate the bandwidth of $\rm CH_B$ for broadcast videos.

B. Multicast-Cost and SI-Based Sorting Operation

The proposed MSFR aims to achieve maximum traffic share by achieving an optimal allocation of the link bandwidth of $\rm CH_B$. To measure the effective amount of shared traffic of a broadcast video, a performance metric that is called multicast-cost ($M_{\rm COST}$) is introduced. The multicast-cost of a broadcast video j is defined as

$$M_{\rm COST}[\text{MG}_j] = (1+\gamma) \cdot S_B[\text{MG}_j] \cdot \text{SI}[\text{MG}_j] \tag{8}$$

where γ is a parameter that is representing the effect of the multicast packet processing burden. Normally, it is possible to assume that $\gamma = 0$ since S_B is linearly proportional to the packet processing burden of the OLT due to an in-flat packet transmission of a video content [12]. However, a different γ can be assumed in the case of a particular video transmission scheme such as dynamic video bandwidth on demand. Thus, the multicast-cost indicates the effective amount of shared traffic that is achievable by a transmission of a broadcast video by $\rm CH_B$.

The multicast agent within the MSFR mechanism adjusts the channel types of the MGs based on the $M_{\rm COST}$ value and SI, which change whenever an ONU joins or leaves the video MG. The OLT delivers broadcast videos to the ONUs through $\rm CH_B$ if space is available. However, if all of the video virtual channels of $\rm CH_B$ are allocated and virtual channel reservation contention occurs, the effectiveness of multicast traffic sharing through $\rm CH_B$ is examined.

First, the multicast agent executes the SI-based sorting by which MGs are ordered by the SI in the MGMT so that $\text{SI}[\text{MG}_i]$ is smaller than $\text{SI}[\text{MG}_{i+1}]$ for an index $i > 0$. Then, it adjusts the channel types of the MGs to ensure that the MGs with large SI values are delivered through $\rm CH_B$. This SI-based sorting guarantees a maximum traffic share if the entire bandwidth of $\rm CH_B$ can be allocated without any unused space. By assuming that there are L kinds of video virtual channel bandwidths that are ordered as $S_{B,1} < S_{B,2} < \cdots < S_{B,L}$, the optimality of the SI-based sorting of MSFR can be proven as follows: If the smallest SI value of the MG that is supported by $\rm CH_B$ is i, as shown in Fig. 4(a), the minimum sum of the $M_{\rm COST}$ values of selected k shared-type MGs ($\text{CT} = S$), which are expressed as $M_{\rm COST}[k - \text{MGs}]$, is yielded as follows:

$$\begin{aligned} &i \cdot S_{B,1} + (i+1) \cdot S_{B,1} + \cdots + (i+k-1) \cdot S_{B,1} \\ &\qquad = \left[i \cdot k + \frac{k \cdot (k-1)}{2} \right] \cdot S_{B,1} \end{aligned} \tag{9}$$

since $S_{B,1}$ is assumed as the minimum video virtual channel bandwidth [15]. Conversely, the maximum $M_{\rm COST}$ value of $\text{MG}_{D,\rm MAX}$, which is the dedicated-type MG ($\text{CT} = D$) of the largest SI value, is equal to $S_{B,L} \cdot (i-1)$. To fairly compare an effective traffic share, index k must be identical to $\lceil S_{B,L}/S_{B,1} \rceil$. Thus, the multicast-cost difference is always positive, which is shown as follows:

$$\begin{aligned} &M_{\rm COST}[k - \text{MGs}] - M_{\rm COST}[\text{MG}_{D,\rm MAX}] \\ &= \left[i \cdot k + \frac{k \cdot (k-1)}{2} \right] \cdot S_{B,1} - S_{B,L} \cdot (i-1) \\ &\geq \left[i \cdot k + \frac{k \cdot (k-1)}{2} \right] \cdot S_{B,1} - S_{B,1} \cdot k \cdot (i-1) \\ &= S_{B,1} \cdot \left[i \cdot k + \frac{k \cdot (k-1)}{2} - k \cdot (i-1) \right] \\ &= S_{B,1} \cdot k \cdot \left(\frac{k+1}{2} \right) \geq S_{B,L} > 0. \end{aligned} \tag{10}$$

Because the maximum $M_{\rm COST}$ difference is assumed, (10) is satisfied for every i, S_B, and k, which proves that SI-based sorting guarantees the maximum $M_{\rm COST}$ of the $\rm CH_B$, i.e., maximum traffic sharing and optimal bandwidth allocation.

C. Channel-Type Swapping Operation

If it is impossible to allocate the entire bandwidth of $\rm CH_B$ to MGs due to bandwidth granularity of the virtual channels, as shown in Fig. 4(b), an optimal traffic share will no longer be guaranteed, and channel utilization decreases. Note that the $M_{\rm COST}$ of $\text{MG}_{D,\rm MAX}$ may be larger than that of MG_j, even with the same amount of bandwidth occupation, i.e., the sum of $S_{\rm unused}$ and $S_{B,2}$ of MG_j is equal to $S_{B,4}$ of MG_{j-1} in Fig. 4(b). In addition, if the SI-based sorting is not achieved, as shown in Fig. 4(c), optimal traffic sharing is also not

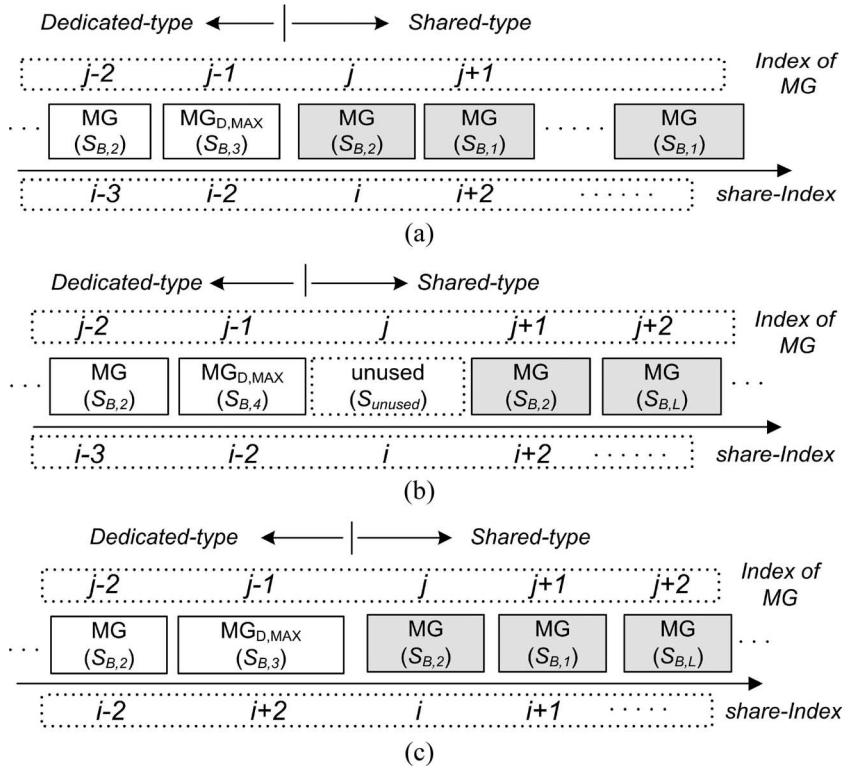

Fig. 4. Cases of SI-based sorting. (a) Entire bandwidth allocation. (b) Unused link bandwidth left: $S_{B,4}$ of $\mathrm{MG}_{j-1} > S_{\mathrm{unused}}$ and $\mathrm{SI}[\mathrm{MG}_{j-1}] < \mathrm{SI}[\mathrm{MG}_j]$. (c) Out-of-order sorting: $S_{B,3}$ of $\mathrm{MG}_{j-1} > S_{B,2}$ of MG_j and $\mathrm{SI}[\mathrm{MG}_{j-1}] > \mathrm{SI}[\mathrm{MG}_j]$.

guaranteed. Thus, to prevent the aforementioned problems, M_{COST} and S_B must simultaneously be considered. The multicast agent in the MSFR guarantees a maximum traffic share and optimal bandwidth allocation by using the following operations.

1) If $S_{\mathrm{unused}} = 0$ and $\mathrm{SI}[\mathrm{MG}_{D,\mathrm{MAX}}] < i$ (the minimum SI value of a shared-type MG), an optimal traffic share for broadcast video delivery is achieved, as proven by (10), and the multicast agent finishes the operation.
2) If $S_{\mathrm{unused}} \neq 0$, $M_{\mathrm{COST}}[\mathrm{MG}_{D,\mathrm{MAX}}]$ is compared with the sum of M_{COST} values of the MGs of the swap-group, where $(S_{\mathrm{unused}} + \sum_l S_B[\mathrm{MG}_l]) \leq S_B[\mathrm{MG}_{D,\mathrm{MAX}}]$, $\mathrm{MG}_l \in$ swap-group. If the former is larger than the latter, the channel types of $\mathrm{MG}_{D,\mathrm{MAX}}$ and the MGs of the swap-group are exchanged. Otherwise, S_{unused} is allocated to as many as possible dedicated-type MGs which have a larger SI than the others, so that the link bandwidth of $\mathrm{CH_B}$ is maximally utilized in a process that is called channel filling.
3) If $S_{\mathrm{unused}} = 0$ and $\mathrm{SI}[\mathrm{MG}_{D,\mathrm{MAX}}] > i$ (out-of-order sorting), $M_{\mathrm{COST}}[\mathrm{MG}_{D,\mathrm{MAX}}]$ is compared with the sum of the M_{COST} values of the MGs of the swap-group on the basis of same bandwidth occupation, as described in 2). Channel-type swapping is executed only if $M_{\mathrm{COST}}[\mathrm{MG}_{D,\mathrm{MAX}}] >$ the total M_{COST} of swap-group.

Even though part of the set of MGs may not be sorted in order, the optimal bandwidth allocation for maximum traffic share and high link utilization is guaranteed. Broadcast video packets have the highest priority in all output ports of the OLT to prevent an out-of-order packet delivery. The pseudocode of the multicast scheduling of MSFR is as follows:

```
begin{
do SI-based sorting and search MG_{D,MAX};
if (S_unused = 0 and SI[MG_{D,MAX}] ≤ i){
   go to end; /* optimal allocation achieved */
else {S_{B,SWAP} ← S_unused, n ← j;
   while (1) {S_{B,SWAP} += S_B[MG_n];
      if (S_B[MG_{D,MAX}] > S_{B,SWAP})
         {Register MG_n to swap-group; n++;}
      else break;}} /* selection of swap-group */
if (∑ M_COST [MGs of swap-group] < M_COST[MG_{D,MAX}])
/* channel-type swapping for optimal traffic share */
   { CT of the MGs of the swap-group ← D;
      CT of MG_{D,MAX} ← S;}
else {n ← j − 2; /* channel filling */
   while (n > 0 and S_unused > 0)
      {/* for dedicated-type MGs */
      if (S_B[MG_n] < S_unused){
      CT of MG_n ← S; S_unused −= S_B[MG_n]; n −−;}}}
} end.
```

An illustrative example of channel-type swapping that uses a comparison of M_{COST} and channel filling for unused parts of $\mathrm{CH_B}$ are shown in Fig. 5. To simultaneously achieve the maximum traffic share and high link utilization that are independent of recursive MSFR operations resulting from abnormal

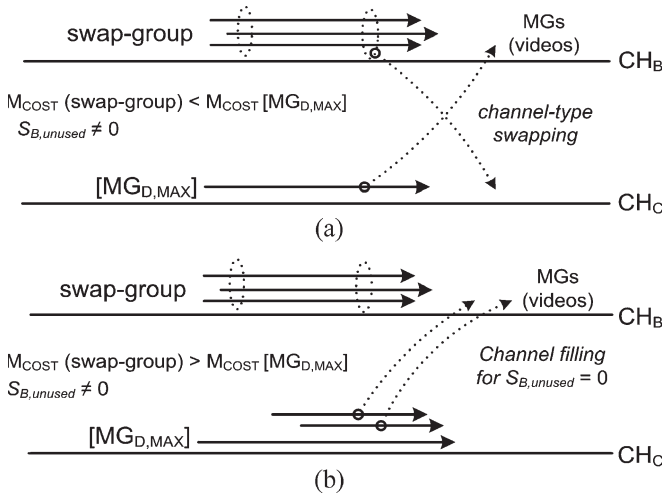

Fig. 5. Channel-type swapping operation. (a) Channel-type swapping with M_{COST} comparison. (b) Channel filling for maximum traffic share.

distribution of MGs, channel-type swapping and channel filling can supplementally be executed by the multicast agent.

D. Discussion

An increase of CAPEX is inevitable in the overlay WDM-PONs and E-PON with an overlay wavelength, due to the deployment of bandpass filters in the ONU side [13], [17]. However, the capability of providing TPSs for the given network conditions, especially broadcast video delivery in the S-WDM-PON, is much superior to the WDM-PON and other overlay WDM-PON since it can support more broadcast videos and unicast applications by using traffic engineering and batch-based multicast. If we consider the ever-increasing multicast traffic in access network and an increase of link speed is the only solution of the WDM-PON for supporting more applications, the S-WDM-PON has promising advantages in terms of cost-effectiveness and service flexibility in the long view, even though the initial CAPEX is higher than that of WDM-PON.

The proposed mechanism can also be applied to the TDM-PON, wherein optical packet broadcasting is naturally achieved. The MSFR can guarantee the maximum multicast traffic share if downstream traffic congestion occurs, so that more broadcast videos are eventually delivered to the customers under the given network conditions. The overall performance of video sharing is almost the same as that of the S-WDM-PON, but the determination of W for optimal video sharing is an important issue. In addition, an improved coordination of bandwidth allocation is required to simultaneously provide types of unicast data services and optimal broadcast video delivery through a single shared link.

Unicast data and broadcast videos are normally multiplexed by TDM at the central office (CO). Our scheduling does not basically mandate the change of data multiplexing in the CO. However, a policy-based scheduling may be needed to achieve a fair link sharing if the MSFR is applied to the TDM-PON OLT. Note that a large part of the link bandwidth must be allocated for the transmission of preference videos in the link from the CO to the ONUs. This implies that the ONU without a video client home eventually receives a smaller amount of bandwidth than other ONUs if traffic congestion occurs from the broadcast videos. This problem is critical in TDM-PON, but rarely affects the performance in the S-WDM-PON due to its dedicated wavelengths. Thus, to provide the ONUs with fair bandwidths, the amounts of allocated multicast bandwidths of ONUs and video sharing status must be considered in packet scheduling and bandwidth allocation at the CO or OLT.

The MSFR mechanism always guarantees a maximum traffic share and optimal bandwidth allocation for changes in a broadcast video demand. This implies that lots of broadcast videos that are destined to a plurality of ONUs can be delivered by the minimum bandwidth in the distribution network, and more unicast applications can be supported. Moreover, the traffic isolation achieved by separating broadcast videos into different data paths improves the QoS. Meanwhile, the S-WDM-PON can also support an asymmetric traffic load. If the downstream traffic load is unevenly distributed, i.e., some ONUs are heavy-loaded and others are not, while the number of broadcast videos being delivered is small, it is possible to allocate the unused link bandwidth of $\mathrm{CH_B}$ to the heavy-loaded ONUs [17]. Note that the MSFR can also be applied to the overlay broadcasting scheme using radio frequency to minimize the inefficiency of the entire video delivery [13]. If the proposed mechanism is applied to an OLT which deploys broadband light sources and some broadband video channels can be shared by the ONUs, then the number of video channels that are needed to support broadcast video delivery, i.e., link bandwidth allocation in the OLT, can be minimized due to the optimal traffic sharing that is achieved by the batch-based multicast, and more unicast applications can be provided to the homes. Moreover, the technical demand of high-order modulation for high-quality video decreases, and the number of broadband sources in the OLT can be effectively reduced.

The performance improvement that is achieved by optimal traffic sharing is significant and independent of the link bandwidth that is provided to the ONU. It is evident that large bandwidth demands that result from ever-increasing HD broadcast video applications cannot always be supported by only network engineering methods, even though the current link bandwidth of the WDM-PON is relatively sufficient. The proposed MSFR mechanism and multicast management achieves a harmonized network design between network engineering and traffic engineering based on the properties of the S-WDM-PON and multicast applications.

IV. Analysis and Results

A. Analysis of Video Virtual Channel Sharing

For analytical simplicity, it is assumed that the amount of video virtual channel bandwidth is equal to S_B in every case. However, if there are L different types of broadcast videos, it is necessary to apply the same analysis to each broadcast video type, which will be L times. A high broadcast video request rate is assumed to clearly validate the effectiveness of video virtual channel sharing through $\mathrm{CH_B}$ at peak time.

1) No Multicast Scheduling: If broadcast videos are delivered to the ONUs only by point-to-point transmission, there is

no virtual channel sharing. This means that the additional link bandwidth of W/N is allocated to a single ONU through $\mathrm{CH_B}$ on average, as discussed. Thus, the number of allocable video virtual channels is the same as $m_B + \inf\{W/(N \cdot S_B)\} = m_B + m_P$, where m_B is the number of virtual channels allocated by $\mathrm{CH_C}$, and the effect of the provisioning of $\mathrm{CH_B}$ on the performance of broadcast video delivery is linear.

2) FCFR Mechanism: Through optical traffic sharing, a few video virtual channels of $\mathrm{CH_B}$ can be shared by the ONUs. The video virtual channel sharing probability for random access (P_S) is derived as $\Pr\{$the same video requested by the home of ONU_i and the home of $\mathrm{ONU}_j \ \ |i \neq j\} = N_{\mathrm{PF}}/N_{\mathrm{BV}}$ from (2). If the number of shared virtual channels of $\mathrm{CH_B}$ follows the binomial distribution [15], the average number of shared video virtual channels is achieved as

$$\Pr\{I\} = \binom{N_W}{i} \cdot P_S^i \cdot (1 - P_S)^{N_W - i} \tag{11}$$

$$E[I] = P_S \cdot N_W = N_W \cdot \frac{N_{\mathrm{PF}}}{N_{\mathrm{BV}}} \tag{12}$$

where N_W is the maximum number of video virtual channels allocable by $\mathrm{CH_B}$. As proven, a preference video requested by a number of homes attached to different ONUs can be supported by a single video virtual channel of $\mathrm{CH_B}$, which can eventually save a large amount of bandwidth in the distribution network. Since at least one video virtual channel has to be provisioned to support a preference video, the average number of shared video virtual channels provided to a single ONU $(m_{\mathrm{sh,FCFR}})$ which can be used to support another broadcast video request is achieved as

$$\overline{m_{\mathrm{sh,FCFR}}} = \frac{N_{\mathrm{PF}}}{N_{\mathrm{BV}}} \cdot N_W \cdot \frac{(I_{S,\mathrm{FCFR}} - 1)}{N} \tag{13}$$

where $I_{S,\mathrm{FCFR}}$ is the average share-index of shared video virtual channels of $\mathrm{CH_B}$, i.e., the average number of member ONUs. Meanwhile, if the effects of the broadcast video request rate and virtual channel provisioning pattern are also considered, the video sharing probability and virtual channel share are affected by λ_B of customers and ρ_B. The N_{PF} is the maximum integer j that satisfies $\lambda_j \cdot L > 1$, while it is not larger than N_{BV}. Because λ_B is the normalized broadcast video request rate of homes during L and $\lambda_j = \lambda_B \cdot p_j$, N_{PF} is derived as $\min(C \cdot \lambda_B, N_{\mathrm{BV}})$.

Note that λ_B is the broadcast video request rate from the large number of homes that are attached to a plurality of ONUs throughout the entire distribution network and are independent of the topological differences of the types of WDM-PONs. By considering that a single ONU segment covers several tens of homes in the case of the prevailing FTTC PON, λ_B is normally large and affects the pattern of broadcast video sharing in the broadcast video server, and it will eventually affect the video virtual channel share in the distribution network among the ONUs.

In this paper, the effectiveness of video virtual channel sharing is validated at a request rate in the range of $\lambda_B < N_{\mathrm{BV}}/C$ to observe the normal behavior of virtual channel sharing while avoiding unnecessary analytic complexity. In the case of saturation of preference videos $(\lambda_B > N_{\mathrm{BV}}/C)$, it is just necessary to substitute $\lambda_B \cdot p_j$ for N_{PF} with N_{BV} in the following equations and analyses. From (2), (12), and (13), $\overline{m_{\mathrm{sh,FCFR}}}$ is derived as follows:

$$\begin{aligned} P_S \cdot N_W &= \frac{N_{\mathrm{PF}} \cdot N_W}{N_{\mathrm{BV}}(\lambda_B, \rho_{\mathrm{PF}})} \\ &= \frac{C \cdot \lambda_B \cdot N_W}{C \cdot \lambda_B + (1 - \rho_{\mathrm{PF}})\lambda_B} \end{aligned} \tag{14}$$

$$\overline{m_{\mathrm{sh,FCFR}}} = \frac{C \cdot \lambda_B \cdot N_W \cdot (I_{S,\mathrm{FCFR}} - 1)}{[C \cdot \lambda_B + (1 - \rho_{\mathrm{PF}})\lambda_B] \cdot N}. \tag{15}$$

In the FCFR mechanism, the video virtual channel of $\mathrm{CH_B}$ can be allocated for the delivery of preference videos only if the allocable virtual channel is free at the time of virtual channel reservation. As a result, preference videos delivered from the server to the OLT with the use of video sharing are randomly distributed over $\mathrm{CH_B}$ and $\mathrm{CH_C}$ by the load of the video request rate, including broadcast video, real-time unicast video, and delayable video. Therefore, the average share-index value of the preference videos that are delivered by $\mathrm{CH_B}$ is the same as the average number of member ONUs of all the broadcast videos that are being supported by the OLT [14]. Thus, $I_{S,\mathrm{FCFR}}$ is derived as

$$\begin{aligned} I_{S,\mathrm{FCFR}} &= \frac{\lambda_B \cdot p_1 + \lambda_B \cdot p_2 + \cdots + \lambda_B \cdot p_{N_{\mathrm{PF}}}}{N_{\mathrm{PF}}} \\ &= \frac{\sum_{j=1}^{N_{\mathrm{PF}}} (\lambda_B \cdot p_j)}{N_{\mathrm{PF}}} = \lambda_B \cdot \frac{\sum_{j=1}^{N_{\mathrm{PF}}} p_j}{N_{\mathrm{PF}}}. \end{aligned} \tag{16}$$

By (2) and the definition of N_{PF}

$$\begin{aligned} I_{S,\mathrm{FCFR}} &= \frac{\lambda_B \cdot \rho_{\mathrm{PF}}}{N_{\mathrm{PF}}} = \frac{\rho_{\mathrm{PF}}}{C} \\ &= \frac{1}{C} \cdot \sum_{j=1}^{N_{\mathrm{PF}}} \frac{C}{j} = \sum_{j=1}^{C \cdot \lambda_B} \frac{1}{j}. \end{aligned} \tag{17}$$

It is evident that the number of member ONUs which share a single video virtual channel cannot be larger than N under any circumstances, and the number of shared video virtual channels cannot be larger than N_{PF}, which is independent of the number of provisioned video virtual channels in $\mathrm{CH_B}$. As a result, the average number of shared video virtual channels that are provided to a single ONU is ultimately yielded as

$$\begin{aligned} \overline{m_{\mathrm{sh,FCFR}}} &= \min\left(\frac{C \cdot \lambda_B \cdot N_W}{[C \cdot \lambda_B + (1 - \rho_{\mathrm{PF}})\lambda_B]}, N_{PF}\right) \\ &\quad \cdot \frac{(I_{S,\mathrm{FCFR}} - 1)}{N} \\ &= \min\left(\frac{C \cdot \lambda_B \cdot N_W}{[C \cdot \lambda_B + (1 - \rho_{\mathrm{PF}})\lambda_B]}, N_{\mathrm{PF}}\right) \\ &\quad \cdot \frac{1}{N} \cdot \left(\min\left(\sum_{j=1}^{C \cdot \lambda_B} \frac{1}{j}, N\right) - 1\right). \end{aligned} \tag{18}$$

3) MSFR Mechanism: Due to the dynamic channel-type swapping, preference videos can occupy the video virtual channels of $\mathrm{CH_B}$ that are independent of the time of virtual channel reservation and network load if that promises an increase of the M_{COST} and high link utilization. Thus, sharing of virtual channels is only restricted by the number of provisioned video virtual channels within $\mathrm{CH_B}$, which is given by N_W. If N_W is larger than the number of preference videos N_{PF}, all of the preference videos can always be delivered to the ONUs through $\mathrm{CH_B}$. In the opposite case ($N_W \leq N_{\mathrm{PF}}$), the number of preference videos that are supportable through $\mathrm{CH_B}$ is equal to N_W at the most. Thus, the average number of shared video virtual channels of a single ONU is derived as

$$\overline{m_{\mathrm{sh,MSFR}}} = \min(N_{\mathrm{PF}}, N_W) \cdot \frac{(I_{S,\mathrm{MSFR}} - 1)}{N}. \tag{19}$$

The average share-index value of those shared video virtual channels $I_{S,\mathrm{MSFR}}$ is also determined by the values of N_W, N_{PF}, and λ_B. Considering the broadcast video request pattern for preference videos, it is evident that $I_{S,\mathrm{MSFR}}$ becomes larger than $I_{S,\mathrm{FCFR}}$ as λ_B increases. If the N_{PF} for a given λ_B is smaller than N_W, all preference videos are delivered to the ONUs by $\mathrm{CH_B}$. Thus, just like the FCFR case, $I_{S,\mathrm{MSFR}}$ is the same as the average number of member ONUs for broadcast videos. Conversely, if N_{PF} is larger than N_W, which occurs if the link bandwidth of $\mathrm{CH_B}$ is too small to support certain numbers of HD videos, $I_{S,\mathrm{MSFR}}$ exceeds the average share-index of preference videos since the MGs with large SI values occupy the virtual channels of $\mathrm{CH_B}$. Moreover, $I_{S,\mathrm{MSFR}}$ converges to N as λ_B increases. From (2), $I_{S,\mathrm{MSFR}}$ can be achieved as follows:

$$I_{S,\mathrm{MSFR}} = \frac{\lambda_B \cdot \rho_W}{N_W} > \frac{\lambda_B \cdot \rho_{\mathrm{PF}}}{N_{\mathrm{PF}}} \tag{20}$$

where

$$\rho_W = \frac{\sum_{j=1}^{N_W} \lambda_j}{\sum_{j=1}^{N_{\mathrm{BV}}} \lambda_j} = \frac{\sum_{j=1}^{N_W} 1/j}{\sum_{j=1}^{N_{\mathrm{BV}}} 1/j} = \sum_{j=1}^{N_W} C/j, \quad N_W < N_{\mathrm{PF}}.$$

Thus, by the same approach applied to (15), (16), and (18), $I_{S,\mathrm{MSFR}}$ is achieved as

$$I_{S,\mathrm{MSFR}} = \min\left(\frac{1}{\sum_{j=1}^{N_{\mathrm{BV}}} \frac{1}{j}} \cdot \sum_{j=1}^{N_W} \frac{1}{j} \cdot \frac{\lambda_B}{N_W},\ N\right). \tag{21}$$

From (17) and (21), the ultimate I_{MSFR} for the given N_W and λ_B is yielded as

$$\begin{cases} \min\left(\sum_{j=1}^{C\cdot\lambda_B} \frac{1}{j}, N\right), & N_{\mathrm{PF}} \leq N_W \\ \min\left(\frac{1}{\sum_{j=1}^{N_{\mathrm{BV}}} \frac{1}{j}} \cdot \sum_{j=1}^{N_W} \frac{1}{j} \cdot \frac{\lambda_B}{N_W}, N\right), & N_{\mathrm{PF}} > N_W \end{cases}. \tag{22}$$

As a result, the average number of shared video virtual channels that are provided to a single ONU in the MSFR is derived as follows from (19) and (22):

$$\begin{cases} C \cdot \lambda_B \cdot \min\left(\sum_{j=1}^{C\cdot\lambda_B} \frac{1}{j}, N\right), & N_{\mathrm{PF}} \leq N_W \\ N_W \cdot \min\left(\frac{1}{\sum_{j=1}^{N_{\mathrm{BV}}} \frac{1}{j}} \cdot \sum_{j=1}^{N_W} \frac{1}{j} \cdot \frac{\lambda_B}{N_W}, N\right), & N_{\mathrm{PF}} > N_W \end{cases}. \tag{23}$$

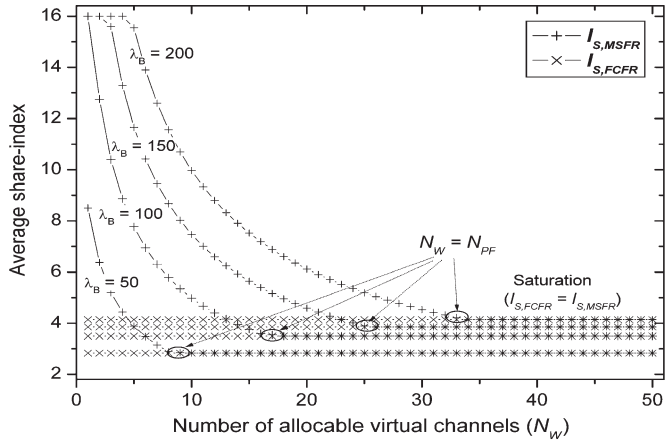

Fig. 6. Average share-indexes of multicast scheduling mechanisms algorithm.

Fig. 6 shows the value of $I_{S,\mathrm{MSFR}}$ that is achieved by (22) for a different λ_B and N_W. In the range of $N_W < N_{\mathrm{PF}}$, wherein only part of the preference videos can be supported by $\mathrm{CH_B}$, the average share-index of the shared video virtual channels of $\mathrm{CH_B}$ goes to N as N_W decreases since the preference videos which have larger SI values occupy the virtual channels of $\mathrm{CH_B}$ by channel-type swapping. Conversely, the value of $I_{S,\mathrm{MSFR}}$ is saturated in the range of $N_W > N_{\mathrm{PF}}$, and it is identical to $I_{S,\mathrm{FCFR}}$, i.e., the average share-index of all the broadcast videos that are being delivered to the OLT, since virtual channel reservation contention does not occur among preference videos. The property of $I_{S,\mathrm{MSFR}}$ heavily affects the economical efficiency of the provisioning of the shared link bandwidth in the S-WDM-PON.

B. Performance of Broadcast Video Sharing

The effectiveness of broadcast video sharing is affected by the number of video virtual channels that are provisioned by $\mathrm{CH_B}$, the video request rate, and the distribution of preference videos. Fig. 7 shows the average number of shared broadcast videos of a single ONU (m_{sh}) versus λ_B. Clearly, m_{sh} increases as λ_B increases for both multicast scheduling mechanisms. This comes from the fact that ρ_{PF} and the average share-index are proportional to λ_B since more broadcast videos are probabilistically preference videos. However, the slopes of the curves differ in both kinds of scheduling mechanisms, and N_W affects the performance of video virtual channel sharing. In the case of the FCFR, an increase in N_W means that more preference videos can probabilistically catch the virtual channels of $\mathrm{CH_B}$ at the time of virtual channel reservation. As a result, the effect of an increase in N_W on virtual channel sharing is manifested, and the video sharing probability gradually increases.

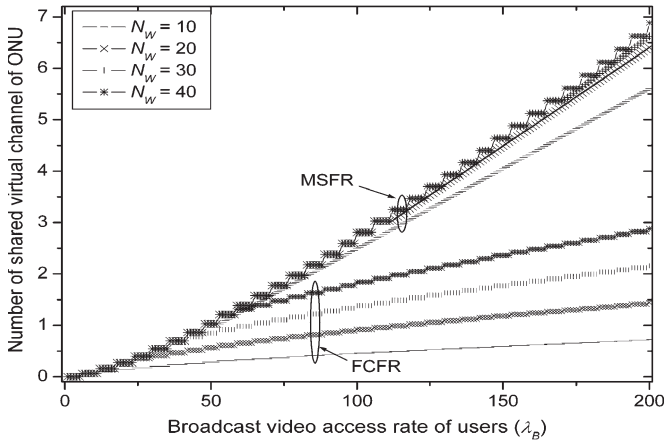

Fig. 7. Average number of shared virtual channels of ONU for λ_B.

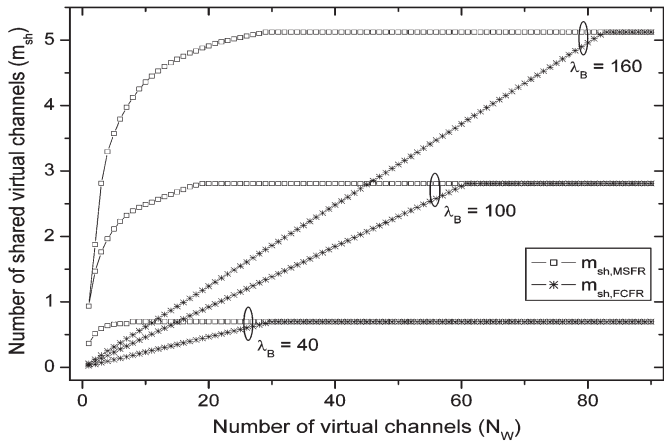

Fig. 8. Average number of shared virtual channels of ONU for N_W.

Conversely, by the dynamic channel-type swapping, the MSFR mechanism always guarantees an effective video sharing, as proven by the large slope, and provides a large number of shared virtual channels, which is over 50% larger than that of the FCFR mechanism for the same N_W. Meanwhile, we observe that $N_W = 30$ is sufficient to achieve a maximum video share since all of the preference videos for the given λ_B can be delivered by $\mathrm{CH_B}$. This property must be considered in the design of the link bandwidth of $\mathrm{CH_B}$.

Fig. 8 shows the average number of shared video virtual channels versus N_W. The value of m_{sh} increases as N_W increases since more broadcast videos can be delivered by $\mathrm{CH_B}$. It also increases as λ_B increases, as discussed. Clearly, the slopes of the curves differ, and the MSFR achieves a peak virtual channel share with a smaller N_W, i.e., a smaller shared link bandwidth that is about one-third of the bandwidth that is required in the FCFR, while guaranteeing an improved video sharing in a transient behavior. However, as the link bandwidth of $\mathrm{CH_B}$ increases by adding video virtual channels, the effectiveness of the MSFR in terms of video sharing decreases; the slope of the curve decreases and ultimately becomes 0. Meanwhile, a small constant slope is maintained up to the peak value because of the random distribution of preference videos in the FCFR. We note that there is an explicit upper bound on the virtual channel sharing for the given condition.

The constant value after the peak represents that provision of additional video virtual channels (link bandwidth) through $\mathrm{CH_B}$ is meaningless from the viewpoint of video sharing. This results from the fact that $I_{S,\mathrm{FCFR}}$ and $I_{S,\mathrm{MSFR}}$ are directly affected by the N_{PF} that is determined by the given λ_B, N, and N_W. The properties of video sharing affect the economic efficiency of the S-WDM-PON, as discussed. Therefore, the effectiveness of virtual channel provisioning must be carefully validated in the process of shared link bandwidth design in order to achieve an optimal video sharing and the most economical network deployment, even though the MSFR reduces the necessity of network engineering such as an increase in the link speed to support more applications.

By considering only the number of virtual channels that must be provisioned by $\mathrm{CH_B}$ to achieve a maximum video share, the explicit upper bound of the FCFR is yielded as

$$\frac{C \cdot \lambda_B \cdot N_W}{[C \cdot \lambda_B + (1-\rho_{\mathrm{PF}}) \cdot \lambda_B]} \leq N_{\mathrm{PF}}$$
$$N_W \leq C \cdot \lambda_B + (1-\rho_{\mathrm{PF}}) \cdot \lambda_B. \tag{24}$$

From (22), the bound of the MSFR is also derived as

$$N_W \leq N_{\mathrm{PF}} = C \cdot \lambda_B. \tag{25}$$

The bound value of N_W represents the approximate optimal number of video virtual channels that are necessary to achieve a maximum broadcast video share, while guaranteeing the economical efficiency of the provisioning of shared link bandwidth for the given λ_B, N, and N_{BV}. We note that the average share-index also affects the performance of broadcast video sharing. From (24) and (25), the rough ratio of the necessary shared link bandwidth in both mechanisms is yielded as

$$\frac{C \cdot \lambda_B + (1-\rho_{\mathrm{PF}}) \cdot \lambda_B}{C \cdot \lambda_B} = 1 + \frac{1}{C} \cdot (1-\rho_{\mathrm{PF}})$$
$$= 1 + \frac{1}{C} - \frac{1}{C} \cdot \sum_{j=1}^{N_{\mathrm{PF}}} \frac{C}{j}$$
$$= 1 + \frac{1}{C} - \sum_{j=1}^{N_{\mathrm{PF}}} \frac{1}{j}. \tag{26}$$

Fig. 9(a) shows the resultant ratios achieved from (26). As λ_B increases, the ratio decreases due to the convergence pattern of the share-index of preference videos. For the same λ_B, a large ratio is achieved with a large N_{BV} (recall that a large N_{BV} directly lowers the virtual channel sharing probability in the FCFR). The results validate the effectiveness and technological compatibility of the MSFR mechanism as a solution to support delivery of a large number of broadcast videos.

The broadcast video sharing of the MSFR mainly increases as λ_B increases, as shown in Fig. 9(b). This is an important property which proves the effectiveness of the proposed MSFR mechanism as a solution to support broadcast applications that are concentrated at peak hours with long service sojourn times.

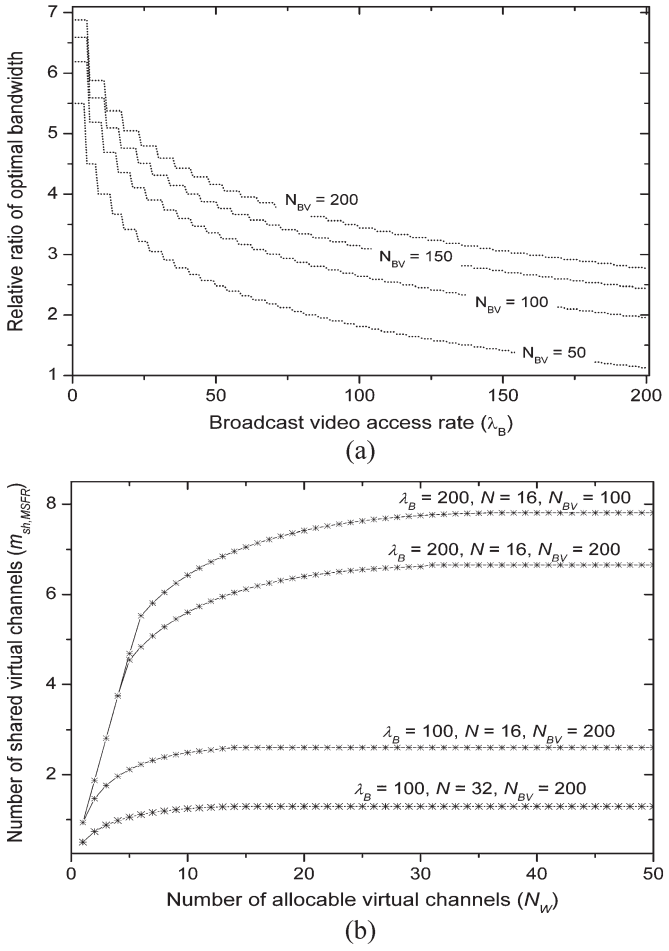

Fig. 9. Performance of video virtual channel sharing. (a) Relative ratio of optimal shared link bandwidth. (b) Effects of N_{BV}, N, and λ_B.

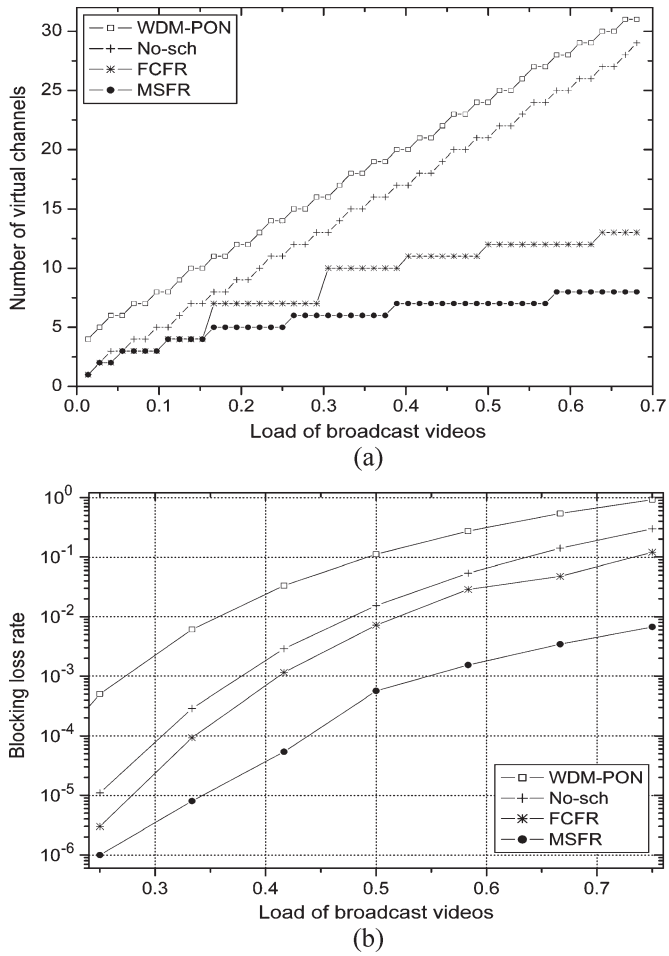

Fig. 10. Performance of broadcast video delivery. (a) Number of necessary video virtual channels of $\mathrm{CH_C}$. (b) Blocking loss rate for 17 provisioned video virtual channels through $\mathrm{CH_C}$.

As shown, N_{BV} and N, i.e., the type of broadcast application and the network scale of the PON, also affect the performance of virtual channel sharing. Recall that the value of the average share-index is restricted by the number of ONUs, even though an ONU consists of a plurality of homes, and the value of N_{PF} is affected by the number of entire broadcast videos that are being delivered to homes. Although their effects on the ultimate performance are rather weak, it is evident that the performance of the MSFR is improved when service density is high, as covered in the previous section.

C. Performance of Video Delivery Service

Broadcast video sharing eventually affects the effectiveness of bandwidth allocation for convergence services. Fig. 10(a) depicts the number of video virtual channels needed to be provisioned through $\mathrm{CH_C}$ to support 15 broadcast videos, with a guaranteed blocking loss rate of $P_{G,B} = 0.0001$. It is assumed that the value of N_W is equal to N_{PF}, which is derived using the numerical methods. Clearly, in every case, the number of necessary video virtual channels increases as the load increases. We note that the slopes of curves significantly differ, and the slope of the MSFR is always the smallest due to maximum video share, which is not directly affected by the changes in broadcast video demand. As a result, broadcast video delivery is always supported with a small number of video virtual channels from $\mathrm{CH_C}$s for the same condition. Therefore, it is possible for the OLT to provide ONUs with a larger link bandwidth for unicast applications.

Conversely, the blocking loss rate of broadcast videos is shown in Fig. 10(b), where the number of video virtual channels of $\mathrm{CH_C}$ is consistently fixed by the administrator. Similar to the previous results, the MSFR mechanism guarantees the smallest slope of blocking loss rate because the multicast agent of the OLT provides the ONUs with more effective video virtual channels through $\mathrm{CH_B}$. If the bandwidth granularity of video virtual channel or λ_B increases, the effectiveness of the MSFR mechanism becomes more significant. These quantitative results clearly validate the advantages of the MSFR mechanism and the S-WDM-PON for convergence services.

D. Performance of the OLT System

The performance of the OLT system is affected by multicast channel scheduling since a large number of packets can be processed in the optical layer. In this section, the transient behavior and performance are investigated apart from the average performance validated in the previous sections. To observe the transient switching performance, S-WDM-PON

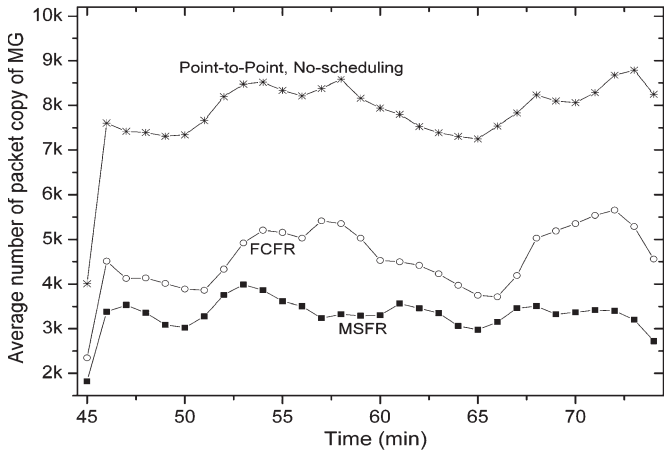

Fig. 11. Average number of packet copies of MG observed every 1 s.

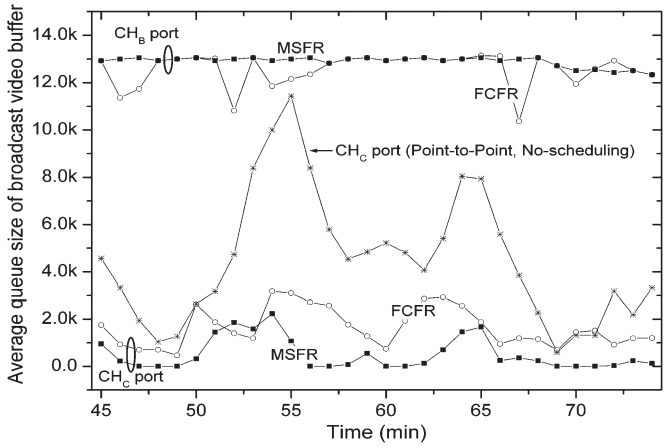

Fig. 12. Average queue size of broadcast buffer observed every 0.01 s.

simulation model and broadcast delivery scenario with IGMP were configured using the OPNET modeler. The simulation parameters and assumptions are as follows: The OLT supports 15 ONUs for $N_{\mathrm{BV}} = 200$, $S_B = 19.2$ Mb/s, $W = 1$ Gb/s, and the N_W for $\mathrm{CH_B} = 45$. The total broadcast video request rate of all the homes attached to a single ONU is a maximum of 16, while the pattern of broadcast video requests follows Zipf distribution in the broadcast video server. The average sojourn time of a home for a single video delivery service is assumed to be 4 min (exponentially distributed) to achieve a clear comparison of transient performance. The advantage of the MSFR over the FCFR becomes more significant if the assumed request rate or sojourn time increases.

The average number of multicast packet copies that are needed to transmit a single broadcast video is shown in Fig. 11. Because all broadcast video packets are delivered to the logical ports of member ONUs by normal multicast switching in the cases of point-to-point and no-scheduling, a large number of packet copies are inevitable. Conversely, the multicast scheduling mechanisms reduce the packet processing burden since the packets of broadcast videos that are transmitted by $\mathrm{CH_B}$ are directly delivered to the logical $\mathrm{CH_B}$ port via a separate path. We note that the MSFR stably maintains the smallest packet processing burden at peak time by sharing preference videos that are heavily requested in the optical layer.

By the reduced number of broadcast video packet transmissions, the average queue size of the broadcast video data buffer of $\mathrm{CH_C}$ port decreases, as shown in Fig. 12. In the instances of point-to-point and no-scheduling, the same number of broadcast video streams as the number of requests must be provisioned since video stream sharing is not permitted, even for the preference videos. The large fluctuation in queue size, which is observed to be from 52.5 to 57.5, results from a large number of broadcast video requests from homes, which eventually results in the degradation of the performance of unicast applications. On the contrary, the proposed mechanism minimizes bandwidth provisioning by combining the requests of homes for preference videos and by achieving the maximum traffic share in the optical layer. Note that part of the $\mathrm{CH_B}$ bandwidth is not utilized in the case of the FCFR. This comes from the fact that unoccupied video virtual channels in $\mathrm{CH_B}$, which results from the end of a video transmission, cannot be reallocated until another broadcast video delivery starts. Conversely, the MSFR algorithm maintains the smallest queue size possible that is independent of the change in video demand. Thus, the service interference of broadcast videos on other applications is minimized, while the link bandwidth of $\mathrm{CH_B}$ is entirely utilized. These properties make possible an economic OLT system and convergence service design.

V. Conclusion

The concept of traffic share-based multicast channel scheduling that is suitable for broadcast video delivery and multicast service in WDM-PONs has been described. Based on the established theoretical foundations of video virtual channel sharing and the share-index, the mathematical analyses of the performance of broadcast video sharing and efficiency of bandwidth allocation in the S-WDM-PON have been achieved, and the design issue of the provisioning of the shared link bandwidth has been discussed. It is clear that the optical overlay broadcast video delivery in S-WDM-PON guarantees the high service efficiency that is necessary to efficiently support convergence services. The proposed MSFR and packet switching mechanism can always support broadcast video delivery with minimum link bandwidth in the distribution network and improve the performance of convergence services. In addition, it minimizes service interferences among types of applications, the multicast packet processing burden, and the system buffer size of the OLT.

However, the effectiveness of virtual channel provisioning has to be validated in the step of shared link bandwidth design to achieve an optimal video share and economic efficiency of the network, since it is affected by the maximum affordable video request rate and properties of the network. The advantages that are achieved through a maximum optical traffic share make possible the effective design of convergence services and an economic OLT system. The qualitative and quantitative performance comparisons have been demonstrated by mathematical analyses and simulations.

REFERENCES

[1] G. Kramer, B. Mukherjee, S. Dixit, Y. Ye, and R. Hirth, "Supporting differentiated classes of service in Ethernet passive optical networks," *J. Opt. Netw.*, vol. 1, no. 8/9, pp. 280–298, Aug. 2002.

[2] G. Kramer, *Ethernet Passive Optical Networks*. New York: McGraw-Hill, 2005.

[3] N. Kim, H. Yun, J. Yoo, T. Kim, B.-W. Kim, and M. Kang, "Performance enhancement of differentiated services in E-PON: Smaller buffer and efficient traffic service isolation," in *Proc. OFC*, Anaheim, CA, Mar. 6–11, 2005, pp. 208–210.

[4] S.-J. Park, C.-H. Lee, K.-T. Jeong, H.-J. Park, J.-G. Ahn, and K.-H. Song, "Fiber-to-the-home services based on wavelength-division-multiplexing passive optical network," *J. Lightw. Technol.*, vol. 22, no. 11, pp. 2582–2591, Nov. 2004.

[5] U. Hilbk, T. Hermes, J. Saniter, and F.-J. Westphal, "High capacity WDM overlay on a passive optical network," *Electron. Lett.*, vol. 32, no. 23, pp. 2162–2163, Nov. 1996.

[6] D. Das, G. Dutta, and D. Datta, "Packet-error rate based power budget for multiple-access WDM networks with subcarrier multiplexed control packets," *IEEE Photon. Technol. Lett.*, vol. 12, no. 3, pp. 359–361, Mar. 2000.

[7] K. S. Kim, D. Gutierrez, F.-T. An, and L. G. Kazovsky, "Batch scheduling algorithm for SUCCESS WDM-PON," in *Proc. IEEE GLOBECOM*, 2004, vol. 3, pp. 1835–1839.

[8] F.-T. An, K. S. Kim, D. Gutierrez, S. Yam, E. Hu, K. Shrikhande, and L. G. Kazovsky, "SUCCESS: A next-generation hybrid WDM/TDM optical access network architecture," *J. Lightw. Technol.*, vol. 22, no. 11, pp. 2557–2569, Nov. 2004.

[9] T. S. Yum and M. Chen, "Dynamic channel assignment in integrated services cable networks," *IEEE Trans. Commun.*, vol. 42, no. 234, pp. 2023–2027, Feb.–Apr. 1994.

[10] Y. W. Leung and T. S. Yum, "Connection optimization for two types of videoconferences," *Proc. Inst. Elect. Eng.—Commun.*, vol. 143, no. 3, pp. 133–140, Jun. 1996.

[11] C. Perkins, L. Gharai, T. Lehman, and A. Mankin, "Experiments with delivery of HDTV over IP networks," presented at the 12th Int. Packet Video Workshop, Pittsburgh, PA, Apr. 2002.

[12] D. Hoffman, G. Fernando, V. Goyal, and R. Civanlar, *RTP Payload Format for MPEG1/MPEG2 Video*, Jan. 1998. RFC 2250.

[13] J.-H. Moon, K.-M. Choi, and C.-H. Lee, "Overlay of broadcasting signal in a WDM-PON," presented at the Optical Fiber Commun. (OFC) Conf., Anaheim, CA, Mar. 5–10, 2006, Paper ThK8.

[14] W. Shu and M.-Y. Wu, "Resource requirements of closed-loop video delivery services," *IEEE Multimedia*, vol. 11, no. 2, pp. 24–37, Feb. 2004.

[15] D. Gross and C. M. Harris, *Fundamentals of Queueing Theory*, 3rd ed. New York: Wiley-Interscience, pp. 56–82.

[16] K. Okamoto, T. Hasegawa, O. Ishida, A. Himeno, and Y. Ohmori, "32 × 32 arrayed-waveguide grating multiplexer with uniform loss and cyclic frequency characteristics," *Electron. Lett.*, vol. 34, no. 22, pp. 1865–1866, Oct. 1997.

[17] H. Song, B. Mukherjee, Y. Park, and S. Yang, "Shared-wavelength WDM-PON access network for supporting downstream traffic with QoS," presented at the Optical Fiber Commun. (OFC) Conf., Anaheim, CA, Mar. 5–10, 2006, Paper OThK2.

[18] J. Nakagawa, N. Suzuki, C. Man, and T. Uo, "Development of optical interfaces for GE-PON PX-20 supporting a 64× split ratio and 20 km transmission range," in *Proc. ECOC*, Sep. 2005, vol. 2, pp. 143–144.

[19] M. D. Vaughn, D. Kozischek, D. Meis, A. Boskovic, and R. E. Wagner, "Value of reach-and-split ratio increase in FTTH access networks," *J. Lightw. Technol.*, vol. 22, no. 11, pp. 2617–2622, Nov. 2004.

[20] L. B. Sofman, B. Krogfoss, and A. Agrawal, "Dimensioning of active broadcast channels in access IPTV network," presented at the Optical Fiber Commun. (OFC) Conf., Anaheim, CA, Mar. 5–10, 2006, Paper JThB75.

[21] J. Wang, L. Sun, X. Jiang, and Z. Wu, "IGMP snooping: A VLAN-based multicast protocol," in *Proc. HSNMC*, Jeju, Korea, Jul. 3–5, 2002, pp. 335–340.

[22] IETF RFC 1112, RFC 2236, *Internet Group Management Protocol Version*, 1989/1998. ver. 1/2.

[23] D. Bertsekas and R. Gallager, *Data Networks*, 2nd ed. Englewood Cliffs, NJ: Prentice-Hall, 1993, pp. 186–206.

NamUk Kim (S'02) received the M.S.E.E. and Ph.D. degrees from the Information and Communications University, Daejeon, Korea, in 2003 and 2007, respectively.

In 2001, he was an Adjunct Researcher with the Optical Ethernet Team, Korea Telecom. From 2002 to 2004, he was with the Broadband Convergence Network Laboratories, Electronics and Telecommunications Research Institute, Korea. He is currently with the Information and Communications University. He has participated in projects that are developing multiple service control agents in wavelength/time division multiplexed-passive optical networks and packet scheduler for adaptive bandwidth allocation and quality of service (QoS) management. His research interests include multicast scheduling, differentiated services network QoS, flow control, and wireless and wired convergence networks.

Minho Kang (S'75–M'77–SM'91) received the B.S.E.E. degree from Seoul National University, Seoul, Korea, in 1969, the M.S.E.E. degree from the University of Missouri, Rolla, in 1973, and the Ph.D. degree from The University of Texas, Austin, in 1977.

From 1977 to 1978, he was with the ATT Bell Laboratories, Holmdel, NJ. From 1978 and 1989, he was a Department Head and a Vice President with the Electronics and Telecommunications Research Institute. In addition, from 1985 to 1988, he served as the Electrical and Electronics Research Coordinator with the Korean Ministry of Science and Technology. In 1990–1998, he was an Executive Vice President with the Korea Telecom, where he was in charge of R and D, quality assurance, and overseas business development groups. In 1999, he joined the Information and Communications University, Daejeon, Korea, as a Professor, served as Dean of Academic and Student Affairs, and has been the Director of the Optical Internet Research Center since 2000. He is the author of *Broadband Telecommunications Technology* (Artech House, 1993).

Dr. Kang was awarded the Order of Merit-DongbaekJang from the Korean Government and the Grand Technology Medal from the 21st Century Management Club in 1983 and 1991, respectively, for his contribution to optical communications technology development. He served as the Study Group Chairman at the Asia Pacific Tele-community of Bangkok during 1996–1999. He is a member of the National Academy of Engineering in Korea. He is an Associate Editor of the *IEEE Optical Communications and Networks* Magazine.